

**ENCIT2020-9999**

**THE EFFECT OF OXYGEN ENRICHMENT ON THE HEIGHT OF NON-  
PREMIXED INVERSE DIFFUSION FLAMES**

**Luisa Dahlem Almeida<sup>a</sup>**  
luisadahelm@gmail.com

**Rodrigo Motta Dartora<sup>a</sup>**  
rodrigodartora98@gmail.com

**Camilo Hoyos Alvarez<sup>a</sup>**  
caanhoal@hotmail.com

**Fernando Marcelo Pereira<sup>a</sup>**  
fernando@mecanica.ufrgs.br

**Andrés Armando Mendiburu Zevallos<sup>a</sup>**  
andresmendiburu@yahoo.es

**Paulo R. Pagot<sup>b</sup>**  
pagot@petrobras.com.br

<sup>a</sup>Federal University of Rio Grande do Sul, Av. Paulo Gama, 110, Porto Alegre.

<sup>b</sup> PETROBRAS – Petróleo Brasileiro S.A.

**Abstract.** *An experimental study was conducted to investigate the effect of oxygen on the height of non-premixed inverse diffusion flames. An experimental setup was used in which a jet of oxidizer was injected into chamber filled with natural gas to form flames on a simple jet burner. The flame height is defined as the distance from the burner outlet to the peak of luminosity intensity on its central line and was determined by an optical technique. Pictures were taken using an ICCD camera while different percentages of oxygen were applied in the oxidant. The height of flame was found to decrease with the enrichment of O<sub>2</sub> and to grow linearly with the flow rate. Also, the effect of O<sub>2</sub> enrichment in the flame temperature and the stoichiometric ratio was investigated.*

**Keywords:** *inverse flames, height, oxygen.*

## 1. INTRODUCTION

Flames can be divided into two main classes: premixed flames and diffusion flames. In the diffusion flames the combustion reaction occurs at the interface between the fuel and the oxidizer where the mixing and reaction processes take place simultaneously. This type of flame is considered safer than the pre-mixed flame, therefore, is commonly used in combustion equipment such as diesel engines and industrial burners (Coelho and Costa, 2007).

Inverse diffusion flames (IDF) are very similar to a normal diffusion flames (NDFs) except that the relative positions of the fuel and oxidizer are exchanged. Recently, there has been a growing interest in the IDF because of its lower soot emission when compared with NDFs (Escudero, 2016). On the other hand, soot and polycyclic aromatic hydrocarbons (PAH) form on the outside of an IDF envelope, in the fuel stream, and escape un-oxidized since they do not pass through the high temperature reaction zone. This is an interesting aspect of these flames, since it may yield information about soot inception and growth, and the formation of soot precursors, such as PAHs (Jung et al, 2012). Besides being an object of study, the IDFs can be used in industrial heating processes, tar conversion into producer gas by a partial combustion reactor (Verhoeven, 2011) and carbon nanotubes production (Xu et al, 2005).

The laminar flame height of a diffusion flame is an important parameter. It has been used to test models of flame structure and to calculate residence times of soot particles (D'anna et al., 2002). In practical terms, the flame height is a fundamental parameter in the design of burners and ovens. The most common definitions of the height of a flame is the distance, on the centerline, from the burner exit to 1) the position where the fuel and oxidizer are in stoichiometric

proportions or 2) the position where the maximum temperature is reached or 3) the position where the flame reaches a peak of luminosity by a certain device.

Wu and Essenhigh (1984) measured the flame height of an IDF by measuring the maximum temperature on the centerline using a thermocouple and Rayleigh scattering technique. Satel and Shah (2018) and Mahesh and Mishra (2010) presented the IDF height as a sum of two heights: the height of the blue zone of the flame - called the premix length - and the height of the region with the highest emission of light called luminous length which is associated with the production of soot. They showed that the maximum concentration of OH lies just at the lean side of the stoichiometric mixture in laminar diffusion flames. Lee et al. (2005), Mikofski (2006) and Zhang et al. (2013) found the height of flame by measuring the peak of the OH \* radical over the centerline using LIF / PLIF images. Finally, Mikofski (2006) also determined the height of flame by measuring the peak blue intensity on the flame axis recorded with an intensified color charge-coupled device (ICCD) camera.

Burke and Schumann (1928) were the first to develop a theoretical analysis for diffusion flames and obtained good results between predicted and measured flame heights of NDFs and IDFs. Roper (1977) extended this theory and obtained the most commonly used correlations for predicting NDF flame heights by adjusting some parameters with experimental results for a large number of normal laminar diffusion flames. Mikofski (2006) made some modifications to Roper's analysis with the aim of adapting it to his measurements of inverse flames. These modifications were used by other researchers as Jung et al. (2012).

The objective of the present work is to measure the flame height of natural gas inverse diffusion flame and its behavior when there is an oxygen enrichment in the oxidant through optical techniques and compare it to previous researches and existing correlations for diffuse flames.

## 2. METHOD

### 2.1 Experimental Setup

The experimental setup used in this experiment is shown in Figure 1. The fuel used in this experiment was natural gas with the following volumetric composition: 90% methane, 5.6% ethane, 1.5% propane, 1.3% carbon dioxide and 1.6% nitrogen (Sulgas, 2018) The flow rate of the fuel and oxidant are measured with electronic mass flow controllers (Bronkhorst) with uncertainties of 0.8% of reading and 0.2% of the full scale. The oxidant is conducted to the combustion chamber through a stainless steel 7,3 mm diameter tube as the fuel is transported through a concentric 50mm x 50mm stainless steel square section duct, in which there is a honeycomb to straighten the flow before it enters a chamber that has two flat borosilicate windows of 200 mm x 40 mm placed on opposite sides allowing the researches to watch the combustion and to take the pictures using an ICCD camera – which is attached to the structure of the experimental bench. Also, there is an ignition system located near to the oxidant-fuel supply to start the combustion. Table 1 lists the air and fuel flow rates for the methane IDFs.

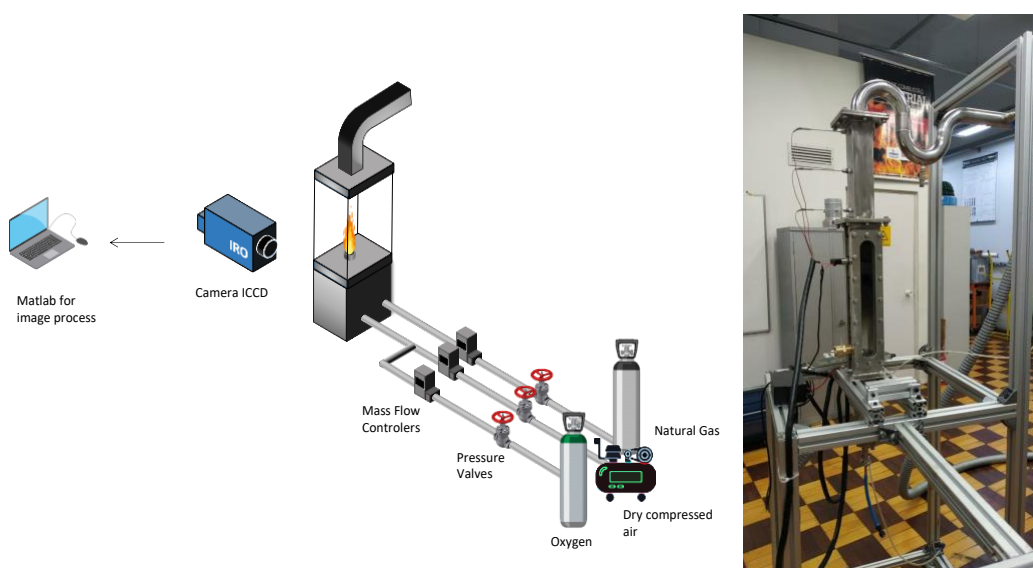


Figure 1. Experimental setup for inverse diffusion flame experiments.

Table 1 – Flow conditions

$Q_f^a$ (slpm)	$Q_o^b$ (slpm)	$X_{O_2}$	$V_f^c$ (c m/s)	$V_o^d$ (c m/s)	$V_o/V_c$	$Re_f^e$	$Re_o^f$
10	1.1	0.21	6.87	45.67	6.64	193	209
		0.28					205
		0.35					205
		0.42					206
		0.21					247
		0.28					242
	1.3	0.35	243				
		0.42	243				
		0.21	286				
		0.28	280				
		0.35	280				
		0.42	280				
	1.5	0.21	324				
		0.28	317				
		0.35	317				
		0.42	318				
		0.21	362				
		0.28	354				
	1.7	0.35	355				
		0.42	355				
		0.21	355				
		0.28	355				
		0.35	355				
		0.42	355				
1.9	0.21	355					
	0.28	355					
	0.35	355					
	0.42	355					
	0.21	355					
	0.28	355					

<sup>a</sup>  $Q_f$ , volume flow rate of fuel (at 298 K and 101 kPa)

<sup>b</sup>  $Q_o$ , volume flow rate of oxidant (at 298K e 101 kPa)

<sup>c</sup>  $V_f$ , average fuel velocity at the chamber

<sup>d</sup>  $V_o$ , average oxidant velocity at the exit of the circular tube.

<sup>f</sup>  $Re_f$ , Reynolds number based on the cold-flow conditions of the fuel and hydraulic diameter of the annular cross section.

<sup>e</sup>  $Re_o$ , Reynolds number based on the cold-flow conditions of the oxidant and internal diameter of the central circular tube.

The height of flame was determined by an optical technique. Pictures were taken using an ICCD camera while different percentages of oxygen were applied in the oxidant, starting at 21%. An ICCD camera directly amplifies the incoming light. The main difference between an CCD and an ICCD camera is that the CCD camera has narrower response in the light spectrum while the ICCD captures, in addition to the visible, part of the ultraviolet and infrared spectrum. The camera used in this experiment captured a wave-length between 255 and 1064 nm. Since the most luminous part of the flame is the soot region, the CCD camera showed images where this region was saturated. The ICCD camera was used not to intensify, but to attenuate while integrating the entire electromagnetic spectrum. This attenuation helped to remove the saturation and to produce an intensity curve. Finally, flame images were recorded at a rate of 3 frames per second for 10 seconds (total of 30 images per flame).

The camera records the light intensity values of the objective under a two-dimensional coordinate system in millimeters, previously calibrated with a standard object of known dimensions. The output is a matrix of 3 columns with the information of position X, position Y and average intensity of the 30 images on a scale of 0-1100 counts. The output data was used to reconstruct the image of the flame by using a MATLAB code as shown in Fig. 2.

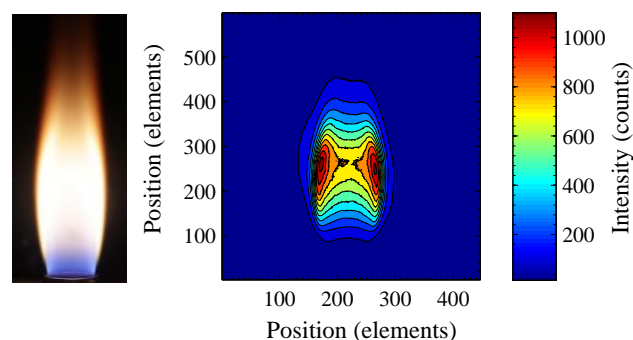
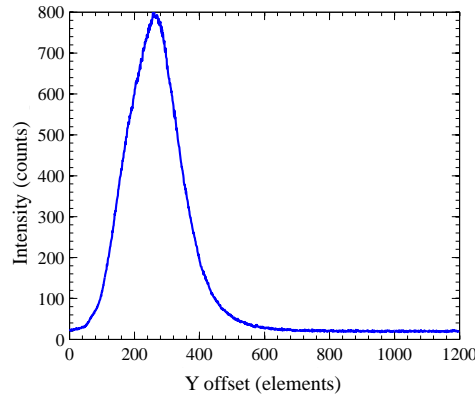


Figure 2. Reconstructed image of a 1.9 l / min GN / flame 42%



a)

Figure 3. Intensity profile over the centerline of a 1.9 l/min GN / flame (42% O<sub>2</sub>)

The flame height is defined as the distance from the burner outlet to the peak intensity on its central line, and can be calculated through the number of elements and their equivalence in millimeters. Figure 3 shows the intensity profile over the centerline for the flame shown in Figure 2.

## 2.2 THEORETICAL ANALYSIS

The Roper et al (1977) theoretical model to calculate the height of flame for circular cross-section burners is given by

$$H_f/Q = [4\pi D_0 \text{Ln}(1 + 1/S)]^{-1} \left(\frac{T_0}{T_f}\right)^{0.67}, \quad (1)$$

where  $H_f$  is the diffusion flame height (cm),  $Q$  is the volumetric flow rate of fuel adjusted to ambient temperature (cm<sup>3</sup>/s),  $D_0$  is the diffusion coefficient at ambient temperature (cm<sup>2</sup>/s),  $S$  is the stoichiometric ratio of oxidizer to fuel volume,  $T_0$  is the ambient temperature (K) and  $T_f$  is the average flame temperature (K). Roper found a linear relationship between  $H_f/Q$  and  $[\text{Ln}(1 + 1/S)]^{-1}$  for different fuels in circular port NDFs. Therefore, taking  $T_f$  and  $D_0$  as constants, an average value for proportionality was found.  $D_0$  was assumed by the authors as the diffusion coefficient of oxygen into nitrogen at ambient temperature ( $T_0 = 293$  K) calculated from Fristrom et al (1965) and  $T_f$  was estimated as 1500K. The final equation found by Roper was

$$H_f/Q = (0.133 \text{ s/cm}^2)[\text{Ln}(1 + 1/S)]^{-1}. \quad (2)$$

Mikofski et al (2006) made some modifications to Roper's analysis with the aim of adapting to inverse flames. These modifications were: 1) define  $Q$  as oxidant volumetric flow rate and 2) define  $S$  as the ratio of fuel to oxidant volume for stoichiometric combustion – which is defined by  $S^* = 1/S$ . First, the experimental data found by Mikofski was compared to Eq. 2 modified for IDF's and did not obtained good results for most of the flames. The experimental data for both methane and ethylene IDFs was used to optimize the Roper's model and both found good agreement for the methane flames – which indicates that there may not exist a general correlation for the height of IDFs. Finally, an approximation by least squares method on the OH PLIF measurements was used to generate a modified Roper's correlation for methane IDFs that is shown below in Eq 3.

$$H_f/Q = (0.150 \text{ s/cm}^2)[\text{Ln}(1 + 1/S^*)]^{-1} \quad (3)$$

## 3. RESULTS AND DISCUSSION

In figure 4 shows the experimental results of flame height obtained through the method of integrated photographs using an ICCD camera for 5 fixed flows: 1.1, 1.3, 1.5, 1.7 and 1.9 l/min. It is possible to observe the linear relationship between the oxidant flow and the flame height. An approximation by least squares of the ICCD camera measurements was also used to find a modified Roper correlation for methane IDFs and is shown in Eq. (4). It is observed that the proportionality constant found is different from the one found by Mikofski et al (2006) for the methane IDFs .

$$H_f/Q = (0.165 \text{ s/cm}^2)[\text{Ln}(1 + 1/S^*)]^{-1} \quad (4)$$

A comparison of Eqs. (1) and (4), using Roper's suggested diffusion coefficient,  $D_0 = 0.20 \text{ cm}^2/\text{s}$  and  $T_0 = 298\text{K}$  gave an estimate of  $T_f = 1079\text{K}$  which is significantly lower than Roper's average temperature of  $T_f = 1500\text{K}$  for normal diffusion flames.

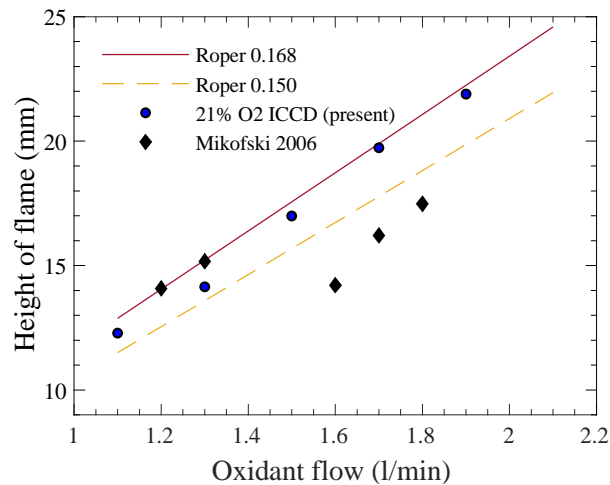


Figure 4. Comparison of flame height measurements with the Mikofski results.

The results obtained in the present study agrees with the hypothesis proposed by Burke & Schumann (1928) and Roper (1977) for laminar diffusion flames - that proposes a linear behavior on the growth of the height of flame as the increase of oxidant flow. Also, it is shown in Fig. 4 that Mikofski et al (2006) measurements for the height of flame are slightly close to a linear increase for low air flow rates (1.1 l/min to 1.3 l/min) and have a discontinuity centered at an air flow rate of 1.6 l/min due to an instability observed in the flames, that have continued to affect the flames above 1.6 l/min. This may explain why they found a different proportionality constant.

The sequency of images shown in Figure 5 corresponds to a series of photographs on IDFs of natural gas and air in the 5 flow conditions analyzed. As noted, the variation in flow within the range (1.1 l / min - 1.9 l / min) does not produce major changes in the appearance of the flame. By contrast, it is possible to notice a considerable variation in size produced by the change of flow in the central oxidant jet. In general, clean air IDFs have well-defined bluish envelopes such as those shown in Figure 5, which allow one to easily measure the length of the reaction zone.

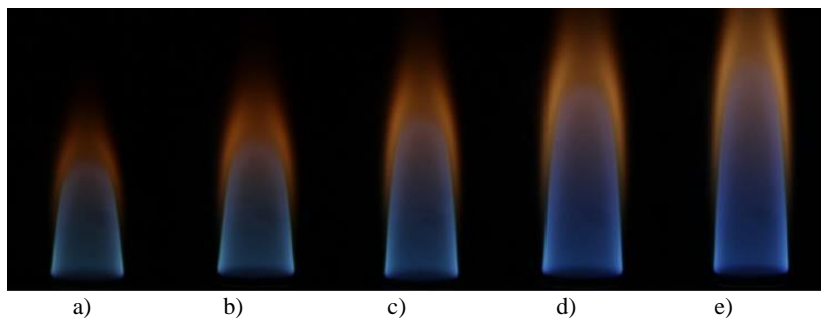


Figure 5. Sequency of photos of a 21% O2 flame with different flow rates of fuel:  
a) 1.1 l/min; b) 1.3 l/min; c) 1.5 l/min; d) 1.7 l/min; e) 1.9 l/min.

Figure 6a shows a comparison between flames with 21% and 35% of O<sub>2</sub> in the oxidizer. By analyzing the Figure 6b, it can be noticed that in flames of pure air a clear peak of luminous intensity is reached where, in the original photograph, is located the tip of the parabola that marks the end of the reaction zone as shown in Figure 6a - it agrees with a consistent value of the flame height. However, when analyzing the 1.9 l / min with 35% O<sub>2</sub> flame shown in Figure 5c, we obtain the intensity profile of Figure 5d which reaches high luminosity values approximately from 10mm, and from that height, there are no major jumps in the curve - that can be seen with the naked eye- that allows one to clearly determine a peak intensity that marks the end of the reaction zone.

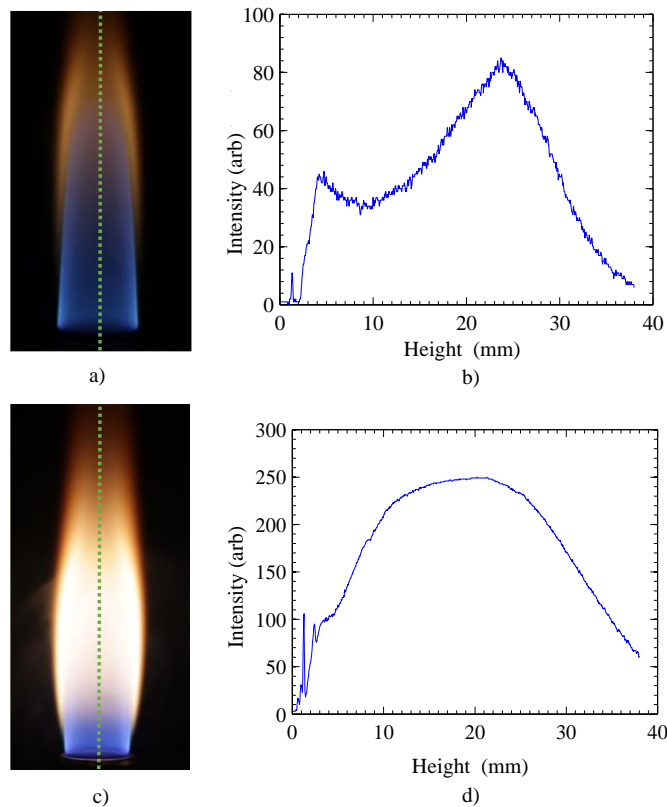


Figure 6. Light intensity analysis: a) Photograph of a 1.9 l / min flame 21% O<sub>2</sub>; b) Profile of intensity on the center line of the filtered photograph of the flame shown in a); c) Photograph of a 1.9 l / min flame 35% O<sub>2</sub>; d) Profile of intensity on the center line of the filtered photograph of the flame shown in c);

Figure 7 shows the ICCD measurements and its behavior when there is an enrichment of oxygen in the oxidizer. It is observed that the results show a decrease in the flame height with the increase of the molar fraction of O<sub>2</sub> in the oxidant and a linear growth with the flow rate in each of the tested oxidant compositions. One can speculate that the increase in O<sub>2</sub> in the oxidizer implies an increase in the flame temperature and consequently an increase in the mass diffusivity of the reactants. Therefore, there is a decrease in the flame height with the enrichment of the air with O<sub>2</sub>. It is also observed that an increase in molar fraction of O<sub>2</sub> within the oxidant composition causes a reduction in the value of the proportionality constant between  $H_f/Q$  and  $[Ln(1 + 1/S^*)]^{-1}$  and, according to the Roper model adapted for IDFs, it means an increase in the adiabatic temperature of the flame and / or a decrease in mass diffusivity as can be observed in Fig. 8. Also, in the case of sooting IDFs, the soot forms are in an annular region outside and above the flame and radiates increasing the luminous flame height and obscuring the blue reaction zone. Despite that, the ICCD camera has shown good performance in the measurements.

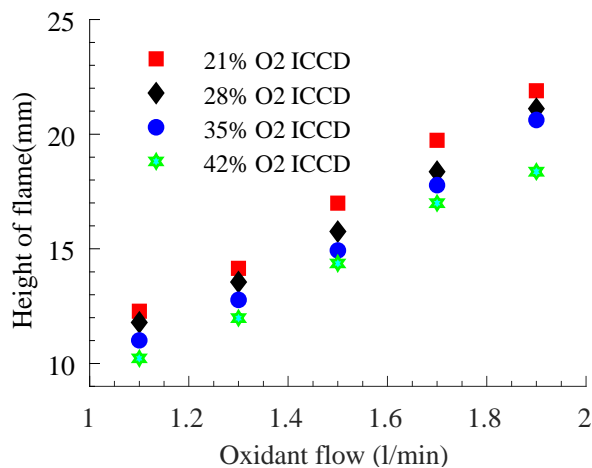


Figure 7. Flame height measurements using an ICCD camera.

On the other hand, when using the adapted correlation given by Eq. (3) an increase of the height of flame was expected as a consequence of the decrease of  $S^*$  - contradicting the experimental measurements found in this research. Escudero et al (2016) also found that although the luminous flame height increases with the increasing O<sub>2</sub>, the reaction zone height decreases almost linearly as the O<sub>2</sub> increases. Demarco et al. (2018) results showed that higher O<sub>2</sub> were found to generate shorter flames, presenting higher temperatures and an increase in the soot production and energy irradiated. Therefore, there is a discrepancy between the results in the literature and the tendency of the model, showing the need for obtaining a specific model for the analysis of IDFs with special considerations such as the inclusion of axial diffusivity terms – which, according to Roper (1977), are important in flames with heights less than 6 times the diameter of the burner, such as those analyzed in this work and all that were possible to stabilize using air /natural gas mixtures. Table 2 presents the variables of the Roper model for IDFs for flames with different O<sub>2</sub>% and allows the calculation of the theoretical height of flame versus the oxidant flow for each O<sub>2</sub>-N<sub>2</sub> mixture.

Table 2 - Variables of the Roper model for IDFs for flames with different O<sub>2</sub>%.

%O <sub>2</sub>	$T_{ad}$ [K]	$D_o$ ( $cm^2/s$ )	$S^*$
21	2226	0.1689	0.103
28	2474	0.1575	0.136
35	2624	0.1471	0.169
42	2727	0.1377	0.201

Figures 8 shows the effect of oxygen enrichment on the mass diffusivity and on the adiabatic flame temperature. The adiabatic flame temperature was calculated using the online software CEARUN provided by NASA. As in the work of Wang et al (2019), the characteristic diffusivity in diffusion flames is that of reactants (here O<sub>2</sub> and CH<sub>4</sub>) into the stoichiometric products (here H<sub>2</sub>O, CO<sub>2</sub>, and N<sub>2</sub>) at 293 K and 1 atm, and was calculated following Bird et al. (1960). It is observed that, as the oxygen enrichment occurs, the adiabatic flame temperature enhances and the mass diffusivity decreases. Escudero et al. (2016) research presents that the oxygen enrichment increases the flame temperature and, consequently, the soot formation rates and this could be verified in this experiment. A higher temperature also provides more oxidation mechanisms and oxidative species that decreases the soot volume fraction. On the other hand, as the oxygen enhances, the mass diffusivity decreases affecting directly the height of flame, as shown in Fig. 7.

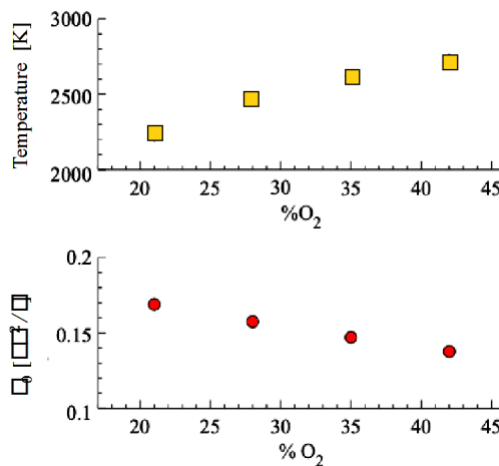


Figure 8. Theoretical analysis of oxygen enrichment effects at the flame temperature and mass diffusivity  $D_0$

#### 4. CONCLUSION

Flame heights of natural gas IDFs were measured by optic techniques for different air flow rates and oxygen enrichment. A linear relationship between the air flow rate and the measured height was observed in coherence with the Roper model. The proportionality value for the Roper's model was adjusted to the experimental results and had good agreement was achieved. On the other hand, adopting all the approaches proposed in the literature, the model fails to reproduce the trend found experimentally in respect to the effect of enriching the oxidant with O<sub>2</sub> on the height of an IDF. While a decrease in flame height was observed with the oxygen enrichment in the oxidant stream, the theory predicts an increase.

## 5. AKNOWLEGMENTS

The authors are grateful to PETROBRAS – Petroleo Brasileiro S. A. for support of this work through Project PT-143.01.12597 (Sigitec 2017/00622-2).

## 6. REFERENCES

- Burke, S.P and Schumann, T. E. W, “Diffusion flames” *Industrial and engineering chemistry*. Vol 20. Page 998
- Coelho, P. and Costa, M., 2007. *Combustão*. Edições Orion, Alfragide, 1st edition.
- Mikofski, MA. Williams, TC. Shaddix, CR. Blevins, LG., 20066. “Flame height measurement of laminar inverse diffusion flames”
- Choi, S, Kim, T, Kim, H, Koo, Kim, J, Kwon, O. “Properties of inverse nonpremixed pure O<sub>2</sub>/CH<sub>4</sub> coflow flames in a model combustor. *Energy*. Vol 93, Pages 1105-1115.
- Escudero et al, 2006. “Effects of oxygen index on soot production and temperature in a ethylene inverse diffusion flame”. *Combustion and flames*, Vol. 146, pp. 63–72.
- Lee, E,J; Oh K.C; Shin, D,H, 2005 “Soot formation in inverse diffusion flames of diluted ethene” *Fuel*. Volume 84, pages 543–550.
- Jung et al, 2012. “The effect of oxygen enrichment on incipient soot particles in inverse diffusion flames”. *Fuel*. Vol. 102. Pages 199–207.
- Mahesh, S. and mishra, D.P, 2010. “Flame structure of LPG-Air inverse diffusion flames in a back step burner”. *Fuel*, Vol. 89, No. 1, pp. 2145–2148.
- Roper, F. G, 1977. “The prediction of laminar jet diffusion flame size: Part I. Theoretical model. *Combustion and flame*. Vol 29. PP. 219-226.
- Roper, F. G, et al 1977. “The prediction of laminar jet diffusion flame size: Part II. Theoretical model. *Combustion and flame*. Vol 29. PP. 227-234.
- Sulgas, Natural gas chemical composition, retrieved november 22, 2018, from Companhia de Gás do Estado do Rio Grande do Sul, <http://www.sulgas.rs.gov.br/sulgas/ficha-tecnica-composicao-quimica>.
- Wu, K.T; Essenhigh, R.H., 1985. “Mapping and structure of inverse diffusion flames of methane”. *Symposium (International) on Combustion*. Elsevier, vol. 50, p. 1925-1932.

## 7. RESPONSIBILITY NOTICE

The authors are the only responsible for the printed material included in this paper.